An event-driven probabilistic methodology for modeling the spatial-temporal evolution of natural hazard-induced domino chain in chemical industrial parks

Men, Jinkun; Chen, Guohua; Yang, Yunfeng; Reniers, Genserik

DOI
10.1016/j.ress.2022.108723

Publication date
2022

Document Version
Final published version

Published in
Reliability Engineering and System Safety

Reliability Engineering and System Safety 226 (2022) 108723

Contents lists available at ScienceDirect

Reliability Engineering and System Safety

journal homepage: www.elsevier.com/locate/ress

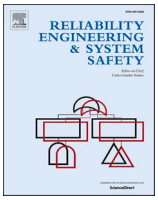

An event-driven probabilistic methodology for modeling the spatial-temporal evolution of natural hazard-induced domino chain in chemical industrial parks

Jinkun Men [a,b], Guohua Chen [a,b,*], Yunfeng Yang [a,b], Genserik Reniers [c,d,e]

[a] Institute of Safety Science and Engineering, South China University of Technology, No.381, Wushan Rd., Tianhe District, Guangzhou 510640, China
[b] Guangdong Provincial Science and Technology Collaborative Innovation Center for Work Safety, Guangzhou 510640, China
[c] Faculty of Technology, Policy and Management, Safety and Security Science Group (S3G), TU Delft, Delft 2628 BX, the Netherlands
[d] CEDON, KULeuven, Campus Brussels, Brussels 1000, Belgium
[e] Faculty of Applied Economics, Antwerp Research Group on Safety and Security (ARGoSS), University of Antwerp, Antwerp 2000, Belgium

ARTICLE INFO

Keywords:
Natural hazard-induced domino chain
Chemical industrial park
Dynamic risk analysis
Disaster chain evolution system
Event-driven probabilistic methodology

ABSTRACT

Natural hazards may rapidly lead to a massive domino chain in chemical industrial parks (CIPs). This work develops a high-efficiency and systematic analytical framework that is applicable to a broad range of uncertain and time-varying factors related to the evolution process of natural hazard-induced domino chain (NHDC). Specifically, the evolution mechanism of NHDC is revealed from a macro-systemic perspective. An event-driven disaster chain evolution system is developed, of which the system state transition is formulated by a Markov decision process and a temporal-difference learning algorithm. A system dynamic risk model is proposed to analyze the dynamic risk associated with NHDC. An earthquake-induced Na-tech scenario is adopted to demonstrate the methodology. Computational results indicate that the proposed methodology is competitive in simulating large-scale system state transition spaces. The involvement of natural hazards would lead to a more complex and severe evolution pattern. Five distinctive stages of the whole NHDC were identified. We found that the value of system dynamic risk is likely to surge in the deterioration stage. Our methodology can dynamically identify the critical system temporal intervals and units at each evolution stage, which has the potential to support the prevention and mitigation of such catastrophic chain events.

1. Introduction

With the advancement of Industry 4.0, chemical industrial parks (CIPs) are becoming larger and more complicated to achieve a higher level of technical functionality [1–3]. A CIP is a typical accident-prone safety-critical system. Natural hazards such as hurricanes, lightning, earthquakes and floods may rapidly lead to a series of loss of containment (LOC) events in CIPs, causing fires, explosions, or toxic cloud emissions [4]. These technological accidents triggered by natural disasters are termed as Na-tech events, which was first coined by Showalter and Myers [5]. Numerous previous studies [6–9] have shown that there appears to be an increase in frequency and severity of Na-tech events. More alarmingly, to realize mutual cooperation, division and modern production, a large amount of hazardous materials are stored, transported, and processed in CIPs, of which a LOC event can cause domino effects and multiple hazards [10]. Up to now, domino effects triggered by natural hazards have imposed tremendous challenges on society, environment, and economy [11]. The typical examples include: the Great East Japan Earthquake in 2011, which caused serious fires and explosions in Sendai and Chiba [9,12]; the Wenchuan earthquake in 2008, which caused the release of over 100 tons of liquid ammonia in Shifang city [13]; and hurricanes “Katrina” and “Rita” in 2005, which caused multiple damages to about 611 industrial installations in Gulf of Mexico [14]. Thus, the analysis of the natural hazard-induced domino chain (NHDC) is essential to ensure safety and continuous production within the chemical process industry.

Recently, the increasing catastrophic destruction associated with Na-tech events has raised the awareness of industries, government and academia [13]. Several countries and regions adopted specific regulations to address Na-tech events, such as *Seveso Directives III* [15],

* Corresponding author.
E-mail address: mmghchen@scut.edu.cn (G. Chen).

https://doi.org/10.1016/j.ress.2022.108723
Received 14 September 2021; Received in revised form 6 July 2022; Accepted 12 July 2022
Available online 13 July 2022

California Accidental Release Prevention [16] and *OECD Guiding Principles for Chemical Accident Prevention, Preparedness and Response* [13]. At present, studies on Na-tech events mainly focus on historical accident statistical analysis [5–7], vulnerability assessment [8,17,18], risk analysis [2,19,20], accident prevention and mitigation [19,21], etc. Advances in lessons learned from past Na-tech events have led to the development of many useful approaches that specifically address hurricane-related Na-tech events, lightning-related Na-tech events, earthquake-related Na-tech events and floods-related Na-tech events [2, 13,20]. According to the past accident analysis, the characteristics of domino chains triggered by different primary hazards are stated in Table 1.

As shown in Table 1, the primary accident scenarios of NHDC may consist of multiple simultaneously failing hazardous installation units (HIUs) [9,12]. The combination of primary accident scenarios is extremely complex and highly uncertain. Moreover, natural disasters can not only cause destructive damage to hazardous installation units (HIUs), but also destroy safety barriers and exacerbate the evolution of domino chains [22]. Thus, the NHDC usually propagates faster than other types of catastrophe chains, which entail the loss of life and property along with negative environmental impacts [1,10]. The accident statistics [23] show that the most frequent technological scenarios in CIPs caused by natural disasters include fires and explosions, of which domino effects are easily triggered. However, most of above research only focuses on installation failures caused by natural disasters and their secondary technological accidents, and rarely considers the propagation of subsequent domino accidents. The main characteristic of domino effects is the expansion and escalation of accident scenarios, linking a primary scenario with one or several higher level scenarios [24]. The traditional quantitative domino risk assessment framework [25] only considers the first propagation level of domino effects. Numerous studies [20,26] have pointed out however that the risk of high-level domino propagation cannot be ignored.

To cope with the complexity of higher level propagations, existing studies were mainly developed on the network graph, of which each involved units can be regarded as a network node, interactions between nodes are modeled by various forms of network arcs [11,27,28]. Another common class of methodologies were based on stochastic simulation, of which the Monte Carlo method [12,26,27,29,30] has been widely used to cope with the complexity of high-level domino propagations. An overview of representative studies for modeling the evolution of domino chains is shown in Table 2. As show in Table 2, research on fire-related accident evolution is abundant. Little attention has been paid to the spatial-temporal evolution of NHDC. Preventing and mitigating such catastrophic chain events are still challenging problems, as the evolution process of NHDC is associated with high uncertainty and complicated dynamic conditions. To sum up, defects in the current research field are mainly reflected in the hereunder detailed three aspects. Firstly, with the expansion of the accident scenarios, two or more hazards (such as earthquakes, hurricanes, floods, fires, explosions, and toxic cloud emissions) may be combined in an isolated, simultaneous, or

Table 1
The characteristics of domino chains triggered by different primary hazards.

Accident Type	Traditional domino chain	Natural hazard-induced domino chain
Hazards	Mechanical failure, Human error, Equipment aging, etc.	Earthquake, floods, hurricane, etc.
Primary Accident Scenarios	Single failure unit	Multiple failure units
Escalation factors	Thermal radiation, Shock wave overpressure, Propellant fragments	Thermal radiation, shock wave overpressure, propellant fragments
Protection measures	Safety barriers functioning	Safety barriers not available

Table 2
An overview of representative studies for modeling the evolution of domino chains.

Authors (Year)	Probabilistic Models	Accident Scenarios	Spatial-temporal Characteristics	Main Work
Khakzad and Reniers [28]	Graph metrics	Domino accidents triggered by fire	Spatial	The vulnerability of process plants was analyzed by graph metrics such as betweenness, out-closeness, and in-closeness in directed graphs, and closeness in undirected graphs. The out-closeness metric was adopted to model the importance of an installation unit to the evolution of domino chain.
Chen et al. [24]	Dynamic Graph	Domino accidents triggered by fire	Spatial-temporal	A methodology involving a domino evolution graph model and a minimum evolution time algorithm was developed to model the spatial-temporal evolution of domino accidents triggered by fire. The synergistic effects and parallel effects of the spatial evolution were considered.
Kamil et al. [31]	Petri-nets	Domino accidents triggered by fire	Spatial-temporal	A generalized stochastic Petri-net model was developed to model the extension likelihood of domino scenarios, which can handle time-dependent failure behavior of the process component in combined loading.
Zeng et al. [32]	Dynamic Bayesian Network	Domino accidents triggered by fire	Spatial-temporal	The dynamic bayesian network was adopted to model the spatial-temporal propagation pattern of domino effects, of which the impact of add-on (active and passive) safety barriers and the

(*continued on next page*)

Table 2 (*continued*)

Authors (Year)	Probabilistic Models	Accident Scenarios	Spatial-temporal Characteristics	Main Work
				synergistic effect of multiple fires were considered.
Huang et al. [12]	Monte Carlo Simulation	Domino accidents triggered by earthquake	Spatial	The Monte Carlo simulation was adopted to model the complicated domino accident scenarios under earthquake. Domino probabilities at different levels were analyzed for specific primary scenario and overall scenarios.
Ovidi et al. [29]	Monte Carlo Simulation	Domino accidents triggered by fire	Spatial	A agent-based stochastic simulation method was proposed to model the evolution of domino effect in the contexts of add-on protections. The transient evolution of multiple scenarios and related synergistic effects, and the effect of safety barriers were considered.
Huang et al. [26]	Monte Carlo Simulation	Domino accidents triggered by fire	Spatial-temporal	A matrix calculation-based Monte Carlo simulation method was proposed to analyze dynamic evolution process of domino effects.
Chen et al. [27]	Dynamic Graph Monte Carlo	Multi-hazard accident scenarios (fires, explosions, and toxic gas diffusion)	Spatial-temporal	A dynamic graph Monte Carlo method was proposed to model the evolution of multi-hazard accident scenarios and assess the vulnerability of humans and installations exposed to such hazards. The potential contribution of explosions in the accident evolution process was specifically concerned.
Zeng et al. [20]	Stochastic Simulation	Domino accidents triggered by flood	Spatial	A comprehensive procedure was developed based on the characteristics of domino effects triggered by floods, and the fragility model, simulation of flow interference, escalation probability estimation, and risk recomposition were combined.
Lan et al. [11]	Static Graph	Domino accidents triggered by hurricane	Spatial	A network-based approach was developed to model the Na-tech related domino effect, which adopted escalation and probability thresholds to reduce the computational complexity.
Men et al. [30]	Stochastic Simulation	Domino accidents triggered by natural hazards	Spatial	Inspired by the multi-source multi-level propagation pattern of domino chain, a Markov process-based accident propagation model was proposed to cope with the uncertain and complex accident scenarios associated with the evolution process of natural hazard-induced domino chain.

chain reaction manner, resulting in the formation of complex domino chains. The involvement of multiple primary accident sources will further aggravate the accident, and the accident scenario will be more complex. The current studies cannot fully address the severe and complex multi-hazard scenarios caused by NHDC.

Secondly, the evolution of NHDC can be regarded as the combination of the danger of hazard-formative factors, the sensitivity of hazard-formative environment, and the vulnerability of hazard-affected objects, which introduce a lot of uncertainties and dynamic conditions into the system response process [3,11]. It is still challenging to incorporate the existing methodologies into the simulation of large-scale system state transition spaces. To cope with the complex and uncertain propagation process of domino effects, a large number of iterations need to be carried out, which is very time-consuming. At last, many existing studies mainly focus on the release of hazardous materials caused by equipment structural damage, ignoring the difference in the accident consequences caused by the failure of different HIUs.

To solve the research gaps mentioned above, this paper aims to provide a high-efficiency and systematic analytical framework that is

applicable to a broad range of uncertain and time-varying factors related to NHDC. In this promotion, an event-driven disaster chain evolution system (ED-DCES) is developed to clarify the accident propagation characteristics. Through capturing a series of discrete system events, the event-driven mechanism of ED-DCES can discretize the complex evolution process into a set of system state sequences with a limited number of timestamps. Then, the Markov decision process is proposed to formulate the accident evolution process, which provides a probabilistic methodology for modeling a discrete-time state-based accident evolution in situations where there are sequential uncertainties. Moreover, a dynamic risk analysis is developed for the system dynamic response process. The reward of each system state is determined by the system risk of the corresponding accident scenario. To overcome the dimension explosion caused by enormous systems states and actions, a temporal-difference learning algorithm (TDLA) is used to obtain the optimal evolution policy. TDLA inherits the advantages of dynamic programming and Monte Carlo simulation, which does not require a complete state sequence for optimization [33]. Although modeling the spatial-temporal evolution of NHDC in CIPs is the main motivation of this work, the proposed methodology has the potential for application to many other complex safety-critical systems. For these complex safety-critical systems, the disturbances in one sub-system may spread to the other one, leading to a disruptive avalanche of subsequent failures [2,3]. Through capturing the dynamic response process of a system subjected to disturbance, the proposed methodology can quickly identify the critical system units and temporal intervals, which can provide support for the enhancement of the safety and reliability of complex safety-critical systems.

The rest of this paper is stated as follows. The development of the ED-DCES is expounded in Section 2. Section 3 introduces the proposed probabilistic methodology. Section 4 provides a case study to demonstrate the proposed methodology. At last, conclusions are drawn in Section 5. This paper an additional Appendix. A list of nomenclature and methodology verification results are available in the Appendix.

2. Event-driven disaster chain evolution system

To analyze the spatial-temporal characteristics of domino effects triggered by natural hazards, an ED-DCES is proposed in this section. The general system dynamic response process is illustrated in Fig. 1. The system activation conditions are equivalent to the occurrence conditions of NHDC. Based on the accident-causing theory [34], the occurrence and development process of industrial accidents affected by natural disasters are analyzed, and the system activation conditions are stated as follows: (1). Natural hazards are regarded as the primary disasters causing failures of HIUs and generating secondary technological hazards; (2). Secondary technological hazards cause adverse effects to adjacent HIUs; (3). The failure energy of hazard units exceeds the failure threshold of HIUs.

As indicated in Fig. 1, natural hazards can produce LOC events in HIUs that store hazardous materials, causing fires, explosions, or toxic cloud emissions [13,23]. The technological hazards such as heat radiation, shock waves, and propellant fragments generated by fires and explosions can easily cause damage to the adjacent HIUs, triggering a domino chain of accident [2,3,30]. Compared with traditional domino chains, the coupling effect of technological accidents and natural disasters can cause more severe casualties, property losses, and environmental pollution [2,3]. For example, natural disasters may damage the safety protection system. Moreover, other critical infrastructures (such as safe passages) and lifelines (such as water supply systems, power systems, etc.) in the accident area may also be affected by natural disasters, which will greatly hinder the efficiency and effectiveness of emergency management [9,12]. The various features of ED-DCES designs are stated in next sub-sections, including the System Units in Section 2.1, the System State in Section 2.2, the Event-driven mechanism in Section 2.3.

2.1. System units

The proposed ED-DCES consists of an operational hazardous installation unit set ($\mathscr{U}_1$), a hazard unit set ($\mathscr{U}_2$), a vulnerable unit set ($\mathscr{U}_3$) and an environment unit set ($\mathscr{U}_4$), i.e.:

$$ED\text{-}DCES = \langle \mathscr{U}_1, \mathscr{U}_2, \mathscr{U}_3, \mathscr{U}_4 \rangle \tag{1}$$

where $\mathscr{U}_1$ refers to the operational HIUs that may cause technological hazards; $\mathscr{U}_2$ refers to the hazard units which can cause adverse effects to vulnerable units and HIUs; $\mathscr{U}_3$ refers to the objectives affected and damaged by hazards, which mainly includes various human crowds; $\mathscr{U}_4$ is closely related to the derivation of hazards, referring to the relationship among the natural environment, the human environment, and the industrial environment, such as meteorological conditions, personnel distribution, management factors, and land-use layout.

2.2. System state

In CIPs, domino effects are mainly propagated among the HIUs [35]. According to the potential technological hazards associated with HIUs

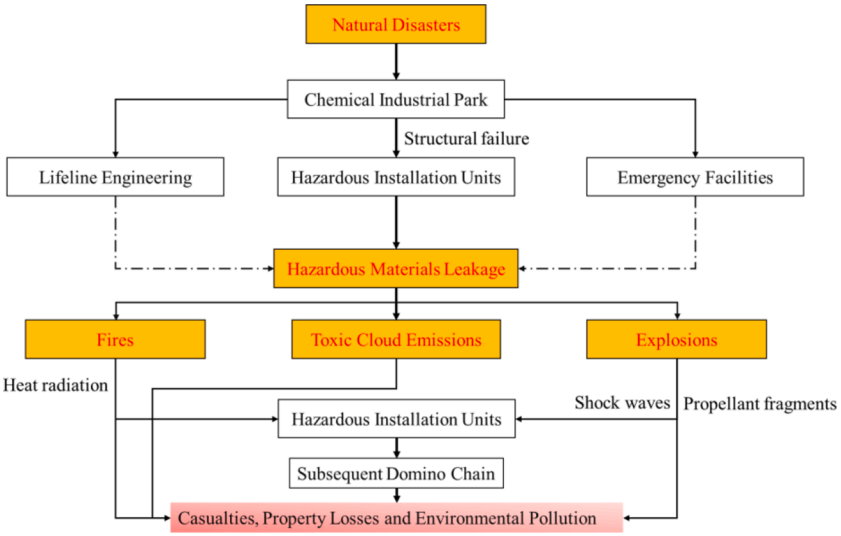

Fig. 1. The general system dynamic response process.

[27,36], five states of HIUs are defined in Table 3.

Suppose that $H = \{h_i | i = 1, 2, \ldots |H|\}$ is the HIU set containing $|H|$ HIUs. The state of system units can be expressed by a state vector $S = (s_1, s_2, \ldots, s_{|H|}) \in \mathscr{S}$. $\mathscr{S}$ is the state space of the proposed ED-DCES.

$$s_i = \begin{cases} 0, \ the\ state\ of\ h_i\ is\ operational \\ 1, \ the\ state\ of\ h_i\ is\ Release \\ 2, \ the\ state\ of\ h_i\ is\ Fire \\ 3, \ the\ state\ of\ h_i\ is\ Explosion \\ 4, \ the\ state\ of\ h_i\ is\ Extingueshed \end{cases} \quad i = 1, 2, \ldots, |H| \tag{2}$$

where s_i is the state of HIU h_i; the operational hazardous installation unit set $\mathscr{U}_1 = \{h_i | s_i = 0\}$; the hazard unit set $\mathscr{U}_2 = \{h_i | s_i = 1 \vee s_i = 2 \vee s_i = 3\}$. System units $\mathscr{U}_1$ and $\mathscr{U}_2$ can be obtained by the state vector S.

2.3. Event-driven mechanism

2.3.1. System event type

In this study, the system dynamic response process is driven by a series of discrete system events. The occurrences of system events cause the corresponding state transition, which in turn updates the system units. According to the event trees provided by Vílchez et al. [36], seven types of events $\Phi = \{\varphi_0, \varphi_1, \varphi_2, \varphi_3, \varphi_4, \varphi_5, \varphi_6\}$ that may occur during the evolution process of NHDC are given in Table 4. The relationship between various system events and system state transitions is shown in Fig. 2.

2.3.2. Discretization procedure of system evolution time

The system evolution time period of ED-DCES Θ is discretized into a set of non-equipotent intervals.

$$\Theta = \{t_0, t_1, t_2, \ldots t_K\} \tag{3}$$

$$t_{k+1} = t_k + \Delta_k, \forall t_k, t_{k+1} \in \Theta \tag{4}$$

$$\Delta_k = \min\left\{\tau_i^k | i = 1, 2, \ldots, |H|\right\}, k = 0,\ 1,\ 2, \ldots, K, \forall \tau_i^k \geq 0 \tag{5}$$

where Θ is the time domain of the whole system dynamic response process; $t_0 = 0$ is the activation time of ED-DCES; t_K is the termination time of ED-DCES. The above discretized time nodes $t_0, t_1, t_2, \ldots t_K \in \Theta$ are used to record the occurrence time of system events. For $\forall h_i \in H$, τ_i^k is its duration of the current state s_i^k. The corresponding event will occur only when the duration of the current state is exhausted. Thus, the system state remains constant for a certain period of time Δ_k, and $\Delta_0, \Delta_1, \Delta_2, \ldots, \Delta_{K-1}$ are denoted as the non-equipotent intervals.

The thermal radiation and shock wave caused by fires and explosions are the main escalation factors with the propagation of domino effects [20]. The technological hazards generated by fires, explosions and leakages are respectively denoted as $\mathscr{F}_k$, $\mathscr{E}_k$ and $\mathscr{Z}_k$, $\mathscr{F}_k$, $\mathscr{E}_k$, $\mathscr{Z}_k \in \mathscr{U}_2^k$. Specifically, the synergistic effect of multiple fires is considered. The thermal radiation intensity μ_f^k and shock wave overpressure μ_e^k received by HIU h_i at time node t_k can be calculated as follows:

Table 3
Five states of HIUs.

System Event Type	Event Description
Operational	The HIU is not failed.
Release	The HIU is physically damaged, resulting in the release of hazardous materials.
Fire	The HIU is on fire, causing heat radiation
Explosion	The LOC event of the HIU induces an explosion, causing heat radiation, causing shock wave overpressure and propellant fragments.
Extinguished	The HIU is failed but does not produce any technological hazards.

Table 4
Seven types of system events.

Event Type	Event Description
Maintain φ_0	The state of HIU does not change at the next time.
Release φ_1	The state of HIU changes from 'Operational' to 'Release' at the next time.
Immediate Ignition φ_2	The state of HIU changes from 'Operational' to 'Fire' at the next time.
Immediate Explosion φ_3	The state of HIU changes from 'Operational' to 'Explosion' at the next time.
Delayed Ignition φ_4	The state of HIU changes from 'Release' to 'Fire' at the next time.
Delayed Explosion φ_5	The state of HIU changes from 'Release' to 'Explosion' at the next time.
Extinguish φ_6	The state of HIU changes from 'Release'/'Fire'/' Explosion' to 'Extinguished' at the next time.

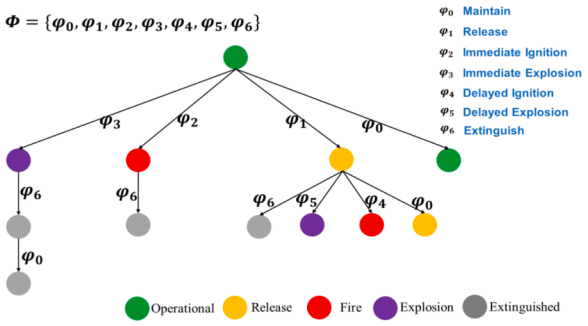

Fig. 2. The relationship between system events and system state transitions.

$$\mu_f^k(h_i) = \sum_{h_j \in \mathscr{F}_k} f_{ji}, h_i \in \mathscr{U}_1^k \tag{6}$$

$$\mu_e^k(h_i) = max\{e_{li} | h_l \in \mathscr{E}_k\}, h_i \in \mathscr{U}_1^k \tag{7}$$

where f_{ji} is the thermal radiation intensity received by HIU h_i from fire hazard $h_j \in F_k$; e_{li} is the shock wave overpressure received by HIU h_i from explosion hazard $h_l \in \mathscr{E}_k$. Assume that $fft(h_i)$ and $eft(h_i)$ are the fire-related escalation threshold and explosion-related escalation threshold associated with HIU h_i, the HIU may fail only when the corresponding thermal radiation intensity $\mu_f^k(h_i)$ or the corresponding shock wave overpressure $\mu_e^k(h_i)$ exceed the escalation thresholds of possible domino effects [37,38]. The following illustrative example shown in Fig. 3 is adopted to demonstrate the fire-related domino effects propagation process.

Illustrative example: Suppose that HIU h_i starts receiving effective heat radiation ($\mu_f^k(h_i) \geq fft(h_i)$, $\mu_e^k(h_i) < eft(h_i)$) at time node t_k. The negative effects associated with fire usually persist for a long time [20]. *ttf* is the "time to failure" of the installation suffering the heat radiation caused by fires. The duration (min) of HIU $h_i \in \mathscr{U}_1^k$ can be obtained as follows [35]:

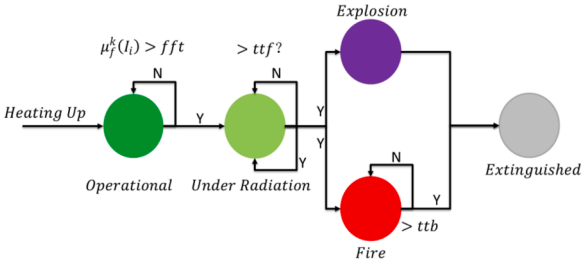

Fig. 3. An illustration of the fire-related domino effects propagation process.

$$\tau_i^k = ttf = \frac{\exp\left(aV_i{}^b + cln\left(\mu_f^k(h_i)\right) + d\right)}{60} \tag{8}$$

where V_i is the volume of HIU h_i; the values of a, b, c, d are stated in Table 5 [35].

According to the superimposed effect model [24], the duration τ_i^{k+1} at the next time node can be obtained as follows:

$$\tau_i^{k+1} = \left(\frac{\mu_f^{k+1}(h_i)}{\mu_f^k(h_i)}\right)^c \left(\tau_i^{k+1} - \Delta_k\right) \tag{9}$$

As shown in Fig. 2, if $\tau_i^{k+1} = 0$, four system events $\varphi_0, \varphi_1, \varphi_2, \varphi_3$ are available for HIU h_i. If HIU h_i is not physically damaged at time node t_{k+1}, i.e., the occurrence of φ_0, the duration remains zero until the state changes. As mentioned above, large-scale natural hazards may greatly hinder the efficiency and effectiveness of emergency management. Thus, if HIU h_i is physically damaged at time node t_{k+1} and causes a fire, i.e., $s_i^{k+1} = 2$, the duration is the burnout time of the fire ($ttb(h_i)$) without human intervention. When the fire duration reaches ttb, the corresponding HIU immediately converts to "Extinguished". For explosion accident $s_i^{k+1} = 3$, $s_i^{k+2}$is transitioned to "Extinguished" instantaneously, i.e., $\Delta_{k+1} = 0$, $t_{k+1} = t_{k+2}$, $s_i^{k+2} = 4$. The state of extinguished HIUs will not change during the subsequent accident expansion, i.e., $\tau_i^{k+2} = \infty$.

An explosion is a rapid expansion in volume associated with an extremely vigorous outward release of energy, usually travels via shock waves [39]. The negative effects of explosions are usually brief and sharp. Thus, if $\mu_e^k(h_i) \geq eft(h_i)$, HIU $h_i \in \mathscr{U}_1^k$ may be physically damaged immediately, i.e., $\tau_i^k = 0$. If HIU h_i is physically damaged at time node t_k and causes a release accident, i.e., $s_i^k = 1$, then τ_i^k is equal to the ignition time it_i^k. Usually, it_i^k is regarded as a random variable [27]. If the ignition time is greater than the release time $rt(h_i)$, then the subsequent fire or explosion will not occur.

Thus, the evolution process of the NHDC can be modeled by the following state matrix $\mathscr{S}$:

$$\mathscr{S} = \begin{pmatrix} S_1 \\ \vdots \\ S_K \end{pmatrix}_{K\times|H|} \tag{10}$$

where $S_k, k = 1, 2, 3, \ldots, K$ is the system state at time node t_k, specifically S_1 is the primary accident scenario caused by Na-tech event; S_K is the termination state of the NHDC. The termination state condition is defined as follows:

$$If\ (\mathscr{T}_k = \varnothing)\ \vee\ (\mathscr{E}_k = \varnothing),\ then\ t_k = t_K \tag{11}$$

3. Probabilistic methodology

The proposed ED-DCES can discretize the complex evolution process into a set of system state sequences with limited number of timestamps. In this section, the sequential uncertainties associated with the discrete-time state-based system dynamic response process can be easily modeled by the Markov decision process. According to the characteristics of multilevel propagation pattern of domino chain [24,30,40], the system dynamic response process can be regarded as a stochastic process with Markov property [30,41], of which the probability distribution of future system states is only determined by the present system state. The independence between non-adjacent system states in the discrete system state sequence can avoid a lot of computational redundancy, which greatly simplifies the difficulty of uncertainty analysis in such dynamic environment.

Formally, the following *Assumption 1* is stated.

Assumption 1. Suppose that the evolution process of NHDC is a Markov process $\{X(t)|t \in \Theta\}$, $\mathscr{S}$ is the stated space, $\forall\ t_1 < t_2 < \ldots < t_k < t$, $x_1, x_2, \ldots, x_k, x \in \mathscr{S}$, the system state $X(t)$ is only related to $X(t_k) = x_k$. Thus, the evolution process of NHDC satisfies the Markov property [30,41], i.e.:

$$P\{X(t) = x|X(t_k) = x_k, \ldots, X(t_1) = x_1\} = P\{X(t) = x|\ X(t_k) = x_k\} \tag{12}$$

According to *Assumption 1*, the system state transition is modeled by the Markov decision process (MDP).

3.1. Markov decision process

MDP provides a probabilistic methodology for modeling a discrete-time state-based accident evolution in situations where there are sequential uncertainties. The proposed MDP consists of six model tuples, which is formulated as follows:

$$MDP = \langle \mathscr{S}, \mathscr{A}, \mathscr{P}, \mathscr{R}, \mathscr{G}, \pi \rangle \tag{13}$$

where $\mathscr{S}$ is the system state space mentioned above; $\mathscr{A}$ is the action space, the occurrence of system event work as the action, $\forall\ a \in \mathscr{A}$ denotes a specific system event set, $S \xrightarrow{a} S'$; $\mathscr{P}$ is the action state probability space; $\mathscr{R}$ is the reward; $\mathscr{G}$ is the return. π is the event occurrence policy. The following *illustrative case* shown in Fig. 4 is adopted to demonstrate the proposed MDP.

Illustrative case: Suppose that $H = \{h_1, h_2, h_3, h_4\}$ is a HIU set containing four HIUs. The system state at time node $t_k \in \Theta$ is denoted as $S_k = (0,1,3,2)$. A_k is denoted as the available system action set at time node t_k. Different actions taken by the system at time node t_k will result in different system states at time node t_{k+1}. When action $a_k = (\varphi_0, \varphi_4, \varphi_6, \varphi_0)$ is adopted, the system state at time node $t_{k+1} \in \Theta$ is $S_{k+1} = (0,2,4,2)$. When $a_k = (\varphi_0, \varphi_2, \varphi_6, \varphi_6)$ is adopted, the system state at time node $t_{k+1} \in \Theta$ is $S_{k+1} = (2,2,4,4)$. With the available system action set A_k and the system state S_k, the event occurrence policy π is defined as follows:

$$\pi(a|S) = P(a_k = a|S_k = S), t_k \in \Theta \tag{14}$$

where $P(a_k = a|S_k = S)$ is the probability of taking action $a \in A_k$ in state S. According to the action taken by the system at time node t_k, the system

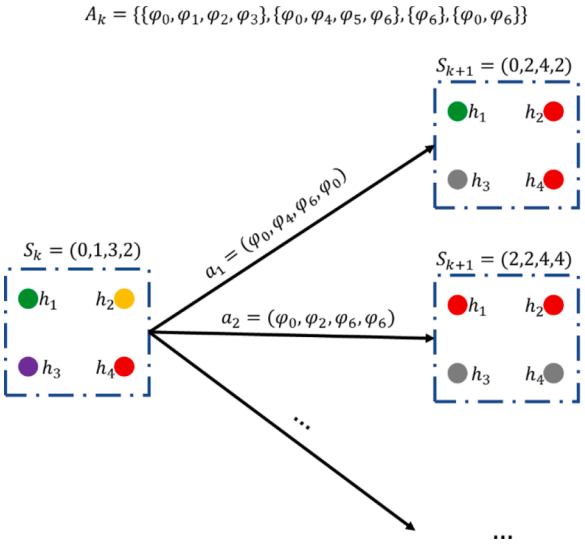

Fig. 4. An illustration of Markov decision process.

Table 5
The values of a, b, c, d [35].

HIU Type	a	b	c	d
Atmospheric	−2.67e-5	1.00	−1.13	9.9
Pressurized	8.845	0.032	−0.95	0

state will be updated accordingly at time node t_{k+1}, i.e. $S \xrightarrow{a} S'$. At the same time (t_{k+1}), the system will receive a reward for taking action a. In this study, the objective of MDP is to determine the optimal event occurrence policy π^*, that is, to identify the riskiest accident evolution pattern. The optimal event occurrence policy π^* can be obtained by maximizing the value function $v_\pi(S)$.

The value function $v_\pi(S)$ is defined as follows:

$$v_\pi(S) = E_\pi\left(R_{k+1} + \gamma R_{k+2} + \gamma^2 R_{k+3} + \ldots + \gamma^{K-k-1} R_K | S_k = S\right) = E_\pi(G_k | S_k = S) \tag{15}$$

where $v_\pi(S)$ is an expect function used to represent the value after taking action in the case of policy π and state S; R_{k+1} is the delayed reward for taking action at time node t_k; $\gamma \in [0,1]$ is the discounted factor. The accumulation of discounted rewards with subsequent state sequence $\{S_k, S_{k+1}, \ldots, S_K\}$ is denoted as the return $G_k = R_{k+1} + \gamma R_{k+2} + \gamma^2 R_{k+3} + \ldots + \gamma^{K-k-1} R_K$. To introduce the value impact of the system action, the action value function is defined as follows:

$$q_\pi(S,a) = E_\pi(G_k | S_k = S,\ a_k = a) \tag{16}$$

According to the formulation of value function $v_\pi(S)$, the following *Bellman equation* can be obtained:

$$v_\pi(S) = \left(R_{k+1} + \gamma R_{k+2} + \gamma^2 R_{k+3} + \ldots + \gamma^{K-k-1} R_K | S_k = S\right) \tag{17.1}$$

$$= E_\pi\left(R_{k+1} + \gamma\left(R_{k+2} + \gamma R_{k+3} + \ldots + \gamma^{K-k-2} R_K\right) | S_k = S\right) \tag{17.2}$$

$$= E_\pi(R_{k+1} + \gamma G_{k+1} | S_k = S) \tag{17.3}$$

$$= E_\pi(R_{k+1} + \gamma v_\pi(S_{k+1}) | S_k = S) \tag{17.4}$$

According to the *Bellman equation*, the recursive relation between adjacent system states S_k, S_{k+1} can be obtained. Similarly, the action value function can be rewritten as follows:

$$q_\pi(S,a) = E_\pi(R_{k+1} + \gamma q_\pi(S_{k+1}, a_{k+1}) | S_k = S, a_k = a) \tag{18}$$

In the context of the event occurrence policy π, the value function $v_\pi(S)$ is actually the expectation of all the action value functions $q_\pi(S,a)$. Thus, the following transformation equations can be obtained:

$$\begin{cases} v_\pi(S) = \sum_{a \in A_k} \pi(a|S) q_\pi(S,a) \\ q_\pi(S,a) = R(S'|S) + \gamma P(S'|S,a) v_\pi(S') \end{cases}, S \xrightarrow{a} S' \tag{19}$$

where $\mathscr{P}(S'|S,a)$ refers to the probability of state S passing to state S' after taking action a. In this study, the state transitions for the corresponding actions are fixed, $S \xrightarrow{a} S'$, thus, $\mathscr{P}(S'|S,a) = 1$. We have:

$$v_\pi(S) = \sum_{a \in \mathscr{A}} \pi(a|S)(\mathscr{R}(S'|S) + \gamma v_\pi(S')), S \xrightarrow{a} S' \tag{20}$$

where $\mathscr{R}(S'|S) = E(R_{k+1}|S,a)$ is the immediate reward for taking action a in state S. In this study, the objective of MDP is to determine the optimal event occurrence policy π^* so as to maximize the value function.

$$v_{\pi^*}(S) = \underset{\pi^*}{argmax} v_\pi(S) \tag{21}$$

3.2. State transition probability

In reality, uncertainty is one of the basic attributes of accident evolution. As a result, many probabilistic models [2,17,25,35] have been developed to present a more realistic assessment by incorporating random characteristics of various risk factors. During the expansion and escalation of accident scenarios, the current system state at time node $t_k \in \Theta$ has a probability of reaching each future system state at $t_{k+1} \in \Theta$, and the probability is called as a transition probability $P_A(S_{k+1}|S_k)$. These basic probabilistic models [2,17,25,35] are adopted to obtain state transition probability values.

3.2.1. The primary accident scenario

According to the system activation conditions mentioned in Section 2, it is assumed that the initial state of the system is safe, i.e.:

$$S_0 = O_{1\times|H|} \tag{22}$$

where S_0 is the initial state of the system, all the entries in the vector S_0 are 0.

For an Na-tech event, HIUs suffer from negative effects imposed by natural hazards. Suppose that $\mathscr{N}$ is a natural hazard unit, the failure probability of HIU $h_i \in H$ under the influence of natural hazard $\mathscr{N}$ is given as follows:

$$P_F^0(h_i) = P(h_i|\mathscr{N}) \tag{23}$$

where $P(h_i|\mathscr{N})$ is the failure probability derived from the vulnerability model. Generally, the vulnerability assessment model [17] is determined by comparing the relationship between the intensity of natural hazards and the resistance of HIUs, which can be expressed as follows:

$$P(h_i|\mathscr{N}) = F(I(\mathscr{N}) > R(h_i)) \tag{24}$$

where $F(\cdot)$ is the mapping relation of the vulnerability model; $I(\mathscr{N})$ is the intensity of natural hazard unit $\mathscr{N}$; $R(h_i)$ is the resistance of HIU h_i. The probabilities of h_i being in five predefined states in the primary accident scenario is given as follows:

$$P_{Na}(S_1(i)) = \begin{cases} 1 - P_F^0(h_i), S_1(i) = 0 \\ P_F^0(h_i) P_T(h_i|R), S_1(i) = 1 \\ P_F^0(h_i) P_T(h_i|F), S_1(i) = 2 \\ P_F^0(h_i) P_T(h_i|E), S_1(i) = 3 \\ 0, S_1(i) = 4 \end{cases} \tag{25}$$

where $P_T(h_i|R)$, $P_T(h_i|F)$ and $P_T(h_i|E)$ are the probabilities of three accident scenarios (release, fire and explosion) after installation failure. In practical engineering application, $P_T(h_i|R)$, $P_T(h_i|F)$ and $P_T(h_i|E)$ can be obtained by the event tree analysis [36]. To sum up, the transition probability of the primary accident scenario can be formulated as follows:

$$P_A(S_1 = (S_1(1), S_1(2), \ldots, S_1(|H|)) | S_0) = \prod_{i=1}^{|H|} P_{Na}(S_1(i)) \tag{26}$$

where $P_A(S_1|S_0)$ is the state transition probability (from S_0 to S_1), $S_1(i)$, $i = 1, 2, \ldots, |H|$ is the state of h_i at time node t_1, $t_1 = 0$ is the activation time of ED-DCES.

3.2.2. The domino accident scenario

The technological hazards that can trigger the domino effects are mainly thermal radiation and shock wave overpressure generated by fires and explosions. The domino extension probability can be obtained by the classical Probit model [25]. During the propagation of domino effects ($t_k \in \Theta,\ k \geq 1$), for the operational HIU $h_i \in \mathscr{U}_1^k$, its failure probability $P_F^k(h_i)$ can be calculated as follows:

$$P_F^k(h_i) = \frac{1}{\sqrt{2\pi}} \int_{-\infty}^{Y-5} e^{-\frac{x^2}{2}} dx \tag{27}$$

where $P_F^k(h_i)$ is the failure probability of HIU h_i at time node t_k; Y is the probit variable, the probit variable of an "average" installation can be calculated using Table 6 [25,35]. The fire included domino effect propagation probability P_{fi}^k and the explosion included domino propagation probability P_{ex}^k of h_i can be obtained by inserting $\mu_f^k(h_i)$ and $\mu_e^k(h_i)$ into the Eq. (27).

Table 6
Probit of domino effects.

Hazard Type	Installation Type	Probit variable
Heat Radiation	Atmospheric Vessel	$Y = 9.25 - 1.85D_1(tff)$
	Pressure Vessel	$Y = 9.25 - 1.85D_2(tff)$
Shock Wave	Atmospheric Vessel	$Y = -9.36 - 1.43ln(\mu_e)$
	Pressure Vessel	$Y = -14.44 + 1.82ln(\mu_e)$

μ_e is the peak static overpressure, kpa; $D_1(tff) = -1.128\ln(\mu_f) - 2.667 \times 10^{-5}\mathscr{V} + 9.87$; $D_2(tff) = -0.97\ln(\mu_f) - 8.835\mathscr{V}^{-0.032}$; μ_f is the heat radiation intensity, kw/m^2; $\mathscr{V}$ is the volume of the installation, m^3.

Thus, the failure probability of HIU h_i at time node t_k can be reformulated as follows:

$$P_F^k(h_i) = 1 - \left(1 - P_{fi}^k\right)\left(1 - P_{ex}^k\right), \forall h_i \in \mathscr{U}_1^k \tag{28}$$

Similarly, the probabilities of the operational HIU $h_i \in \mathscr{U}_1^k$ being in five predefined states at the next time node t_{k+1} can be calculated as follows:

$$P_{D_1}(S_{k+1}(i)) = \begin{cases} 1 - P_F^k(h_i), S_{k+1}(i) = 0 \\ P_F^k(h_i)P_T(h_i|R), S_{k+1}(i) = 1 \\ P_F^k(h_i)P_T(h_i|F), S_{k+1}(i) = 2, k \geq 1, h_i \in \mathscr{U}_1^k, \tau_i^k = 0 \\ P_F^k(h_i)P_T(h_i|E), S_{k+1}(i) = 3 \\ 0, S_{k+1}(i) = 4 \end{cases} \tag{29}$$

For these units in the "Release" state $\mathscr{Z}_k = \{h_j | S_k(j) = 1\}$, their state transition probabilities can be calculated as follows:

$$P_{D_2}(S_{k+1}(j)) = \begin{cases} P_T(h_i|NC), S_{k+1}(i) = 1 \\ P_T(h_i|DF), S_{k+1}(i) = 2, k \geq 1, h_i \in \mathscr{Z}_k, \tau_i^k = 0 \\ P_T(h_i|DE), S_{k+1}(i) = 3 \end{cases} \tag{30}$$

where $P_T(h_i|DF)$ and $P_T(h_i|DE)$ are probabilities of delayed ignition and delayed explosion events, $P_T(h_i|NC)$ is the probability of no subsequent deterioration after the occurrence of a release accident. Three probability parameters can be obtained by using event tree analysis [36].

To sum up, the transition probability of can be formulated as follows:

$$P_A(S_{k+1}|S_k) = \prod_{h_i \in \mathscr{U}_1^k} P_{D_1}(S_{k+1}(i)) \prod_{h_j \in \mathscr{Z}_k} P_{D_2}(S_{k+1}(j)), k \geq 1 \tag{31}$$

It is worth mentioning that the shock wave overpressure caused by the explosion is a kind of instantaneous damage. For the unit in the explosion state, it will be directly converted to the extinguished state in the next level of the accident scenario, and it will no longer participate in the subsequent accident evolution process.

3.3. Model reward

The evolution process of NHDC is often accompanied by the amplification of uncontrolled energy. Uncontrolled energy may cause serious damage to vulnerable units. According to the traditional quantitative risk assessment (QRA) framework [25], a risk value can be quantified as the product of accident consequence and accident probability. To involve the negative effects of associated with NHDC, the reward of MDP is defined as follows:

$$\mathscr{R}(S_{k+1} = S' | S_k = S) = P_A(S_{k+1} = S' | S_k = S) P_H(S_{k+1} = S') \tag{32}$$

$$P_H(S_{k+1} = S') = \frac{1}{|\mathscr{U}_3|} \sum_{u_i \in \mathscr{U}_3} \left(1 - \left(1 - P_{fdeath}\right)\left(1 - P_{exdeath}\right)\left(1 - P_{todeath}\right)\right) \tag{33}$$

where the state transition probability $P_A(S_{k+1} = S' | S_k = S)$ can be obtained by Eqs. (26) and (31); $P_{fdeath}, P_{exdeath}$ and $P_{todeath}$ are the death probabilities of vulnerable unit, suffering fires, explosions and toxic cloud emissions; $P_H(S_{k+1} = S')$ is the average individual death probability under the influence of a hazard unit set $\mathscr{U}_2^{k+1}$, the probit variable of human injury Y is stated in Table 7 [25].

According to the value function mentioned above, the proposed MDP comprehensively considers the current reward and subsequent delayed rewards. Thus, the riskiest accident evolution pattern is obtained in terms of the accident probability and the accident consequence.

3.4. System dynamic risk model

This work expands the traditional QRA framework to further analyze the dynamic risk associated with the system dynamic response process. Following the Markov property mentioned in *Assumption 1*, the value of system dynamic risk at time $t_k \in \Theta$ is determined by the riskiest system state S_{k+1} at next time node $t_{k+1} \in \Theta$. Thus, the following system dynamic risk model is defined:

$$Risk(S_k = S) = \max\{P_H(S_{k+1} = S')P_A(S'|S) | a \in A_k\}, S \xrightarrow{a} S'; S, S' \in \mathscr{S} \tag{34}$$

where $Risk(S_k = S)$ is the system dynamic risk at time $t_k \in \Theta$; $P_A(S'|S)$ is the system state transition probability from S to S'; $P_H(S_{k+1} = S')$ is the average individual death probability caused by the system state S' at time node t_{k+1}, which is adopted to measure the consequence associated with S'. According to the available system action set A_k at time node t_k, all potential system states at time node t_{k+1} can be obtained. Through comparing the product of state transition probability $P_A(S'|S)$ and death probability $P_H(S_{k+1} = S')$, the riskiest system state S_{k+1} at next time node $t_{k+1} \in \Theta$ can be identified, and the corresponding product is regarded as the value of system dynamic risk at current time node t_k.

3.5. Temporal-difference learning algorithm

To overcome the dimension explosion caused by enormous systems states and actions, a temporal-difference learning algorithm (TDLA) is used to obtain the optimal evolution policy. TDLA is a model-free algorithm, which inherits the advantages of dynamic programming and Monte Carlo to predict the state value and optimal policy [33]. The purpose is to obtain the optimal policy. Specially, the return G_k is approximate as follows:

$$G_k = R_{k+1} + \gamma v(S_{k+1}) \tag{35}$$

where R_{k+1} is the reward at time node t_{k+1}; $v(S_{k+1})$ is the state value of S_{k+1}.

Since TDLA does not require a complete state sequence, the iterative equations for the value function are defined as follows:

$$v(S_k) = v(S_k) + \alpha(G_k - v(S_k)) \tag{36}$$

$$q(S_k, A_k) = q(S_k, A_k) + \alpha(G_k - q(S_k, A_k)) \tag{37}$$

where $\alpha \in [0, 1]$ is the step size. According to the above equations, when TDLA reaches the next state S_{k+1}, the state value of S_k can be estimated.

Table 7
Probit of human injury.

Hazard Type	Probit variable
Heat Radiation	$Y = -14.9 + 2.56ln(6 \times 10^{-3}\mu_f^{1.33}\tau_e)$
Shock Wave	$Y = 5.13 + 1.37ln(\mu_e)$
Toxic Cloud Emission	$Y = \alpha + \beta ln(C^\theta \tau_e)$

Y is the probit variable of human injure. C is the concentration of toxic gasses, ppm; τ_e is the exposure time, minute. α, β and θ are constants describing the toxicity.

4. Case study

An illustrative case study is stated in this section. As shown in Fig. 5, a chemical storage tank farm extracted from an industrial cluster in South China is adopted to be the application scenario. The abandoned tank area in Fig. 5 is not considered in this case study. Thus, ten internal floating roof tanks (T1-T10) are considered in the case study. The geographical distribution of the ten tanks is shown in Fig. 5, of which the ten tanks are labeled as T1-T10 in Fig. 5. The information of the ten storage tanks is stated in Table 8. Moreover, a vulnerable unit is considered in the case study, and the vulnerable unit is located at the yellow dot in Fig. 5. An earthquake-induced accident scenario is adopted to demonstrate the proposed methodology.

The relevant parameters are set as follows: the annual average temperature is 21.3 °C; the annual average wind speed is 1.5 m/s; the average annual relative humidity is 83%; the atmospheric stability is B; the peak ground acceleration (PGA) of earthquake is 0.4 g. According to the damage probability model provided by Campedel et al. [42], the fragility of equipment under the predefined PGA is stated in Table 8. Results indicate that the primary accident scenario damaged by an earthquake most likely includes multiple simultaneous accidents. Three primary accident scenarios are developed for comparison. The proposed methodology is performed on Matlab R2021a under a computer that is equipped with Intel(R) Core(TM) i7-8750H CPU @ 2.20 GHz and 8.00 GB RAM. After some preliminary observations, the step size of TDLA is set to 0.01.

4.1. Accident consequence intensity calculation

The flash point of diesel is close to 55 °C at room temperature, which is a flammable, low volatility liquid material. Delayed ignition is not considered because flammable clouds are not generated, due to the low volatility [43]. The flash point of gasoline is less than 22 °C at room temperature, which is thus a flammable and volatile liquid. In the event of delayed ignition a flash fire or explosion can occur [36]. The corresponding event trees are shown in Fig. 6. The pool fire scenario and vapor cloud explosion scenario are adopted to quantify accident consequences, the related heat radiation intensity and shock overpressure are obtained by using the *PHAST 8.21* consequence modeling software. Calculation results are shown in Tables 9 and 10.

4.2. System event timeline analysis

In this work, the accident propagation process is represented by a series of discrete system events. The proposed methodology can provide a clear-cut system event timeline to capture the spatial-temporal characteristics of NHDC. The corresponding system event timelines are shown in Fig. 7. As shown in Fig. 7(a), for primary accident scenario I, T5 failed under the influence of earthquake, causing a fire, i.e. $S_1 = (0,0,0,0,2,0,0,0,0,0)$, $t_1 = 0$ *min*. At system evolution time $t_2 = 5.91$ *min*, T4 failed due to the thermal radiation from T5, resulting in a release

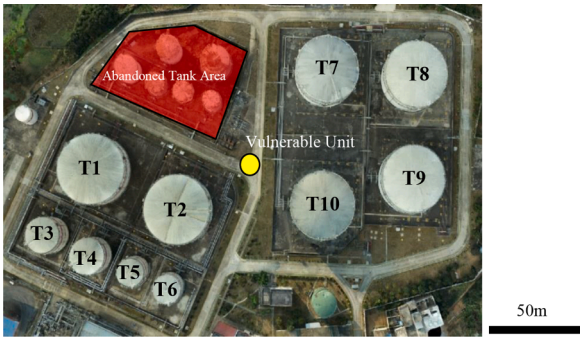

Fig. 5. Chemical Storage Tank Farm.

Table 8
Information of the storage tanks (Unanchored).

No.	Storage Materials	Volume	Storage temperature, pressure	Filling Ratio	Fragility ($\geq DS_2$)	Fragility (DS_3)
T1	Gasoline	20,000 m^3	NPT	0.72	0.931	0.236
T2	Diesel	20,000 m^3	NPT	0.54	0.931	0.236
T3	Gasoline	5000 m^3	NPT	0.85	0.931	0.236
T4	Gasoline	5000 m^3	NPT	0.91	0.931	0.112
T5	Gasoline	3000 m^3	NPT	0.85	0.931	0.236
T6	Gasoline	3000 m^3	NPT	0.65	0.931	0.236
T7	Diesel	20,000 m^3	NPT	0.64	0.931	0.236
T8	Diesel	20,000 m^3	NPT	0.70	0.931	0.236
T9	Gasoline	20,000 m^3	NPT	0.82	0.931	0.236
T10	Diesel	20,000 m^3	NPT	0.56	0.931	0.236

NPT: Normal Pressure and Temperature; *DS* is the damage state of storage tanks, DS_1, corresponding to a minor release; DS_2, corresponding to a relevant release of hazardous materials; and DS_2, for a sudden loss of containment of the entire vessel inventory.

accident. At system evolution time $t_3 = 5.97$ *min*, a delayed ignition event occurred at T4, resulting in a fire accident. At system evolution time $t_4 = 6.16$ *min*, T6 failed due to the thermal radiation from T5 and T4, resulting in a release accident. At system evolution time $t_5 = 6.46$ *min*, a delayed ignition event occurred at T6, resulting in a fire accident. At system evolution time $t_6 = 7.47$ *min*, T2 failed due to the thermal radiation from T5, T4 and T6, resulting in a release accident. No immediate ignition event occurred after the failure of T2. For diesel tank T2, a delayed ignition is not considered because flammable clouds are not generated, due to the low volatility [43]. Thus, in the subsequent evolution, T2 was regarded to be in the extinguished state. At system evolution time $t_7 = 9.20$ *min*, T3 failed due to the thermal radiation from T5, T4 and T6, resulting in a release accident. At system evolution time $t_8 = 9.86$ *min*, a delayed ignition event occurred at T3, resulting in a fire accident. At system evolution time $t_9 = 9.87$ *min*, T1 failed due to the thermal radiation from T5, T4, T6 and T3, resulting in a release accident. At system evolution time $t_{10} = 19.77$ *min*, a delayed ignition event occurred at T1, resulting in a fire accident. In the subsequent evolution process ($t_{11\sim15}$), the accidents extinguished gradually, and all the failed tanks convert to the extinguished state at $t_{15} = 1914.77$ *min*. The final accident scenario I included 6 failed tanks (T1–T6) with 5 fires.

As shown in Fig. 7(b), for primary accident scenario II, T5 and T10 failed under the influence of the earthquake, causing 2 simultaneous fires, i.e. $S_1 = (0,0,0,0,2,0,0,0,0,2)$, $t_1 = 0$ *min*. As shown in Fig. 7(c), for primary accident scenario III, T4, T6 and T10 failed under the influence of earthquake, causing 3 simultaneous fires, i.e. $S_1 = (0,0,0,2,0,2,0,0,0,2)$. Similarly, diesel tanks (T2, T7 and T8) that do not ignite immediately after failure were regarded to be extinguished. Both final accident scenario II and III included 10 failed tanks (T1–T10) with 7 fires. According to the event trees shown in Fig. 6, in this case study, the probability of immediate ignition event is low so as the explosion accident. Thus, there are almost no immediate ignition events and explosion accidents in the obtained system event timelines.

According to the spatial-temporal characteristics of NHDC, the whole evolution process is divided into five distinctive stages: the Na-tech stage E_0, the derivation stage E_1, the domino stage E_2, the deterioration stage E_3 and the extinguish stage E_4. At the Na-tech stage E_0, natural hazards produced LOC events, resulting in primary accident scenarios that may

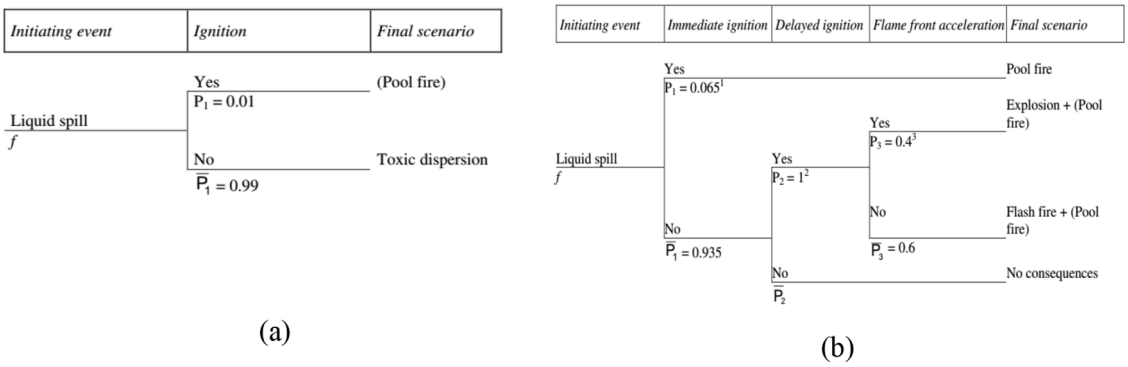

Fig. 6. The corresponding event trees of diesel and gasoline [36], (a) diesel; (b) gasoline.

Table 9
Heat radiation intensity received by Tj or Vulnerable Unit (VU) from Ti (kW/m^2).

Ti/Tj	T1	T2	T3	T4	T5	T6	T7	T8	T9	T10	VU
T1	/	12.19	13.76	11.20	8.72	5.03	1.50	0.61	0.83	1.92	2.96
T2	10.83	/	5.16	9.11	12.67	13.55	2.12	0.94	1.47	4.69	7.46
T3	12.23	5.16	/	27.92	9.11	5.04	0.74	0.54	0.54	0.94	1.47
T4	11.20	10.47	31.43	/	31.43	11.54	1.04	0.61	0.83	1.92	2.39
T5	8.72	14.26	10.47	31.43	/	31.43	1.05	0.61	1.04	2.86	3.35
T6	5.03	15.25	5.90	11.54	31.43	/	1.26	0.65	1.26	4.21	3.78
T7	1.33	2.12	0.74	0.74	0.94	0.94	/	11.17	4.92	6.58	4.02
T8	0.54	0.94	0.54	0.54	0.54	0.55	11.17	/	9.35	4.22	1.82
T9	0.83	1.71	0.61	0.83	1.04	1.26	5.77	10.66	/	12.58	2.86
T10	1.52	4.69	0.94	1.52	2.35	3.57	6.58	4.22	11.17	/	9.35

Table 10
Overpressure received by Tj or Vulnerable Unit (VU) from Ti (kPa).

Ti/Tj	T1	T2	T3	T4	T5	T6	T7	T8	T9	T10	VU
T1	/	17.55	20.24	15.93	12.13	7.70	3.68	2.50	2.65	4.19	5.43
T2	/	/	/	/	/	/	/	/	/	/	/
T3	11.82	5.26	/	30.25	8.66	5.17	1.62	1.17	1.33	2.02	2.41
T4	6.53	6.01	19.98	/	21.61	6.72	1.22	0.89	1.08	1.77	2.05
T5	6.06	10.15	7.21	26.58	/	28.99	1.60	1.17	1.49	2.64	2.98
T6	3.41	9.49	3.77	7.03	24.72	/	1.44	1.09	1.50	2.98	2.77
T7	/	/	/	/	/	/	/	/	/	/	/
T8	/	/	/	/	/	/	/	/	/	/	/
T9	2.79	4.17	2.34	2.77	3.13	3.62	8.84	15.89	/	19.25	5.52
T10	/	/	/	/	/	/	/	/	/	/	/

include multiple simultaneous technological hazards. At the derivation stage E_1, the adjacent HIUs were exposed to the heat radiation, shock waves, and propellant fragments generated by fires and explosions, but no domino accident occurred for the time being. At the domino stage E_2, the primary accident propagated to nearby HIUs, triggering one or more secondary events resulting in overall sequences more severe than those of the primary accident. At the deterioration stage E_3, a delayed ignition event occured, which accelerated the expansion and escalation of domino effects. At the extinguish stage E_4, the accident scenario tended to be stable, and each hazard unit gradually changed into the extinguished state.

The time interval of evolution stage is shown in Table 11. For scenario I, the time interval of E_1 is 0–5.91 min; the time interval of E_2 is 5.91–9.87 min; the time interval of E_3 is 6.46–19.77 min; the time interval of E_4 is 19.77–1914.77 min. For Scenario II, the time interval of E_1 is 0–5.52 min; the time interval of E_2 is 5.59–18.60 min; the time interval of E_3 is 6.82–18.60 min; the time interval of E_4 is 18.60–1905.75 min. For Scenario III, the time interval of E_1 is 0–2.73 min; the time interval of E_2 is 2.73–15.94 min; the time interval of E_3 is 3.25–15.94 min; the time interval of E_4 is 15.94–1901.99 min.

Since the main escalation and expansion of accident scenario occured at evolution stages E_1, E_2 and E_3, the system evolution time associated with the accident expansion is stated in Fig. 8. At the end of the accident evolution, the system states of scenario II and Scenario III are the same. However, the evolution of scenario III is more intense, which is reflected in the system evolution time shown in Fig. 7(c). This indicates that the primary accident scenario has a significant impact on the accident evolution pattern.

As mentioned above, natural hazards such as hurricanes, lightning, earthquakes and floods may rapidly lead to a series of LOC events in CIPs. At the Na-tech stage E_0, the primary accident scenario caused by natural hazards usually consists of multiple primary accident sources. The variation trend of heat radiation intensity received by different tanks is stated in Fig. 9. The increase of heat radiation intensity shows a tendency to become more and more intense. This suggests that the propagation process of domino effects is intensifying as the accident evolves. The experimental results indicate that the synergistic effects associated with multiple simultaneous technological hazards can significantly accelerate the evolution of accidents. The proposed methodology can effectively handle the severe and complex multi-hazard scenarios caused by NHDC.

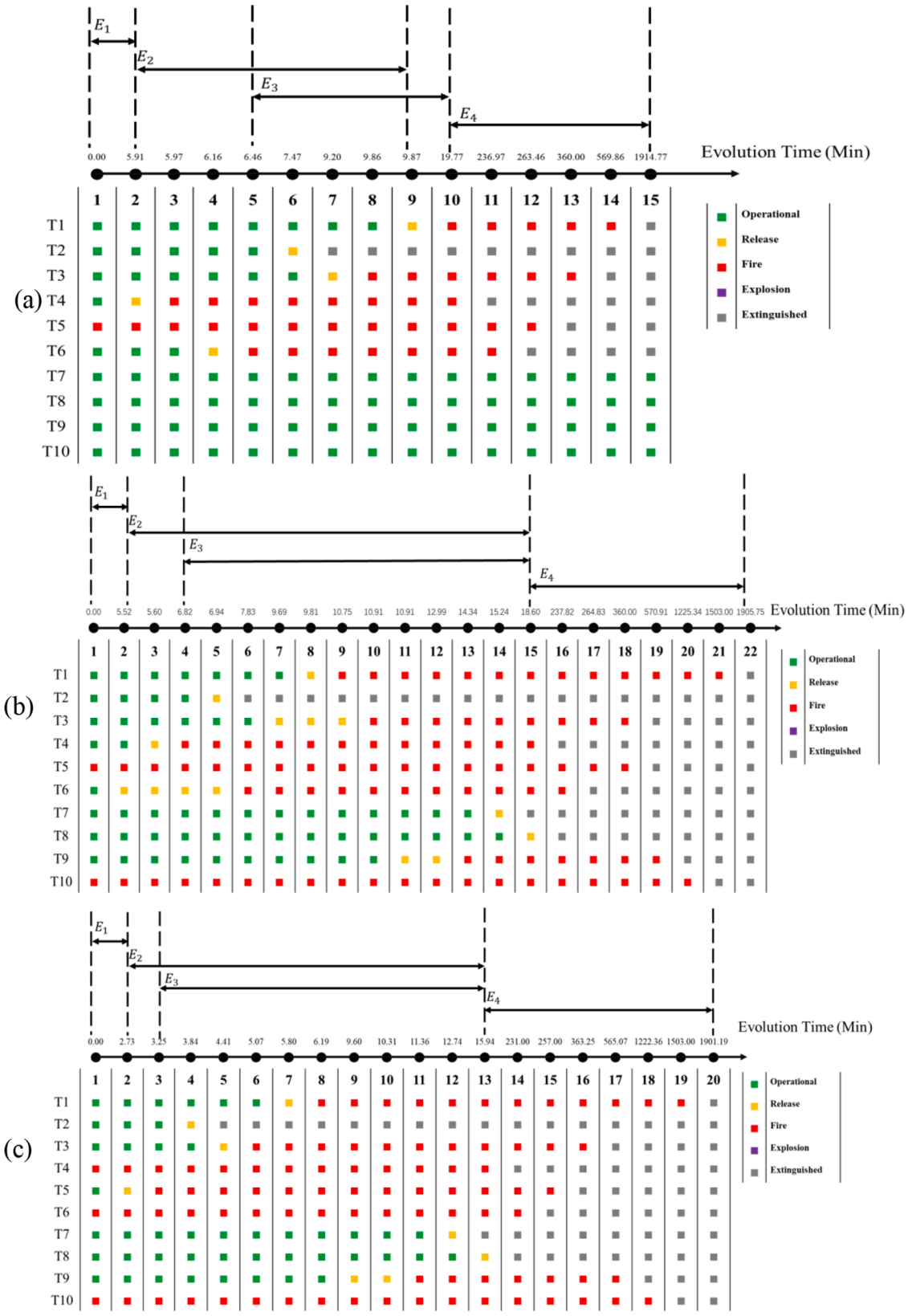

Fig. 7. System event timeline, (a) Scenario I; (b) Scenario II; (c) Scenario III.

4.3. System dynamic risk analysis

In this section, the proposed system dynamic risk model is adopted to further analyze the dynamic risk associated with the system dynamic response process, and analysis results are stated in Tables 12–14. The risk value less than 1.000e-20 is approximate to 0. For scenario I shown in Table 12, at system evolution time $t_2 = 5.91$ *min*, the critical system unit is T4, as it has received effective thermal radiation for more than its

Table 11
Analysis of spatio-temporal characteristics of system dynamic response.

Evolution stages	Scenario I	Scenario II	Scenario III
E_1	0–5.91 min	0–5.52 min	0–2.73 min
E_2	5.91–9.87 min	5.59–18.60 min	2.73–15.94 min
E_3	6.46–19.77 min	6.82–18.60 min	3.25–15.94 min
E_4	19.77–1914.77 min	18.60–1905.75 min	15.94–1901.99 min

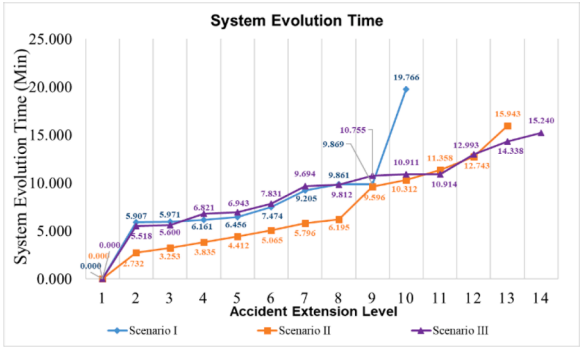

Fig. 8. System evolution time for different primary accident scenario.

ttf. According to the available system action set A_2 at time node t_2, six system events $\varphi_0, \varphi_1, \varphi_2, \varphi_3, \varphi_4, \varphi_5$ may occur to change the state of T4. Through comparing the product of state transition probability $P_A(S_2 = S^{'}|S_1 = (0,0,0,0,2,0,0,0,0,0))$ and death probability $P_H(S_2 = S^{'})$, the riskiest event is immediate ignition φ_2 and the riskiest system state S_2 is identified to be $S_2 = (0,0,0,2,2,0,0,0,0,0)$. The corresponding product $P_H(S_2)P_A(S_2|S_1) = 1.541\text{e}-14$. It is worth noting that $S_2 = (0,0,0,2,2,0,0,0,0,0)$ is regarded as the riskiest system state without the consideration of subsequent evolution process, as it can only be used to determine the value of system dynamic risk at time t_1.

According to the event trees shown in Fig. 6, the probability of the immediate ignition event is relatively low compared to the delayed ignition event. To obtain the riskiest accident evolution pattern, the accumulation of discounted rewards with subsequent state sequence is involved in the value function $v_\pi(S)$. Thus, in the obtained system event timeline shown in Fig. 7(a), $S_2 = (0,0,0,1,2,0,0,0,0,0)$. At system evolution time $t_3 = 5.97\ min$, the critical system unit is still T4. According to the available system action set A_3 at time node t_3, two system events φ_4, φ_5 may occur to change the state of T4. Through comparing the product of state transition probability $P_A(S_3 = S^{'}|S_2 = (0,0,0,1,2,0,0,0,0,0))$ and death probability $P_H(S_3 = S^{'})$, the riskiest event is delayed ignition φ_3 and the riskiest system state S_3 is identified to be $S_3 = (0,0,0,2,2,0,0,0,0,0)$. The delayed ignition event of the failure unit is also taken into account when calculating the risk. Thus, the corresponding risk value rapidly increases to 4.958e-03. As shown in Tables 12–14, such risk surge caused by delayed ignition events generally occurs during the evolution of NHDC. For diesel tanks T2, T7 and T8, the delayed ignition event is not considered, thus the corresponding risk values are relatively low. The risk analysis results are consistent with the obtained system event timelines. The deterioration stage E_3 is the critical temporal interval for the prevention and mitigation of the NHDC, and the gasoline tanks (T5, T6, T1, T9, T4, T3) with high risk values should be allocated more emergency resources.

In reality, the evolution mechanism of NHDC is very complex and associated with high uncertainty and spatio-temporal dynamics. According to the experimental results, the proposed methodology can model the spatio-temporal evolution of the entire NHDC in 20–30 s. Therefore, in practical applications, we can quickly identify the critical system units and temporal intervals according to real accident scenarios.

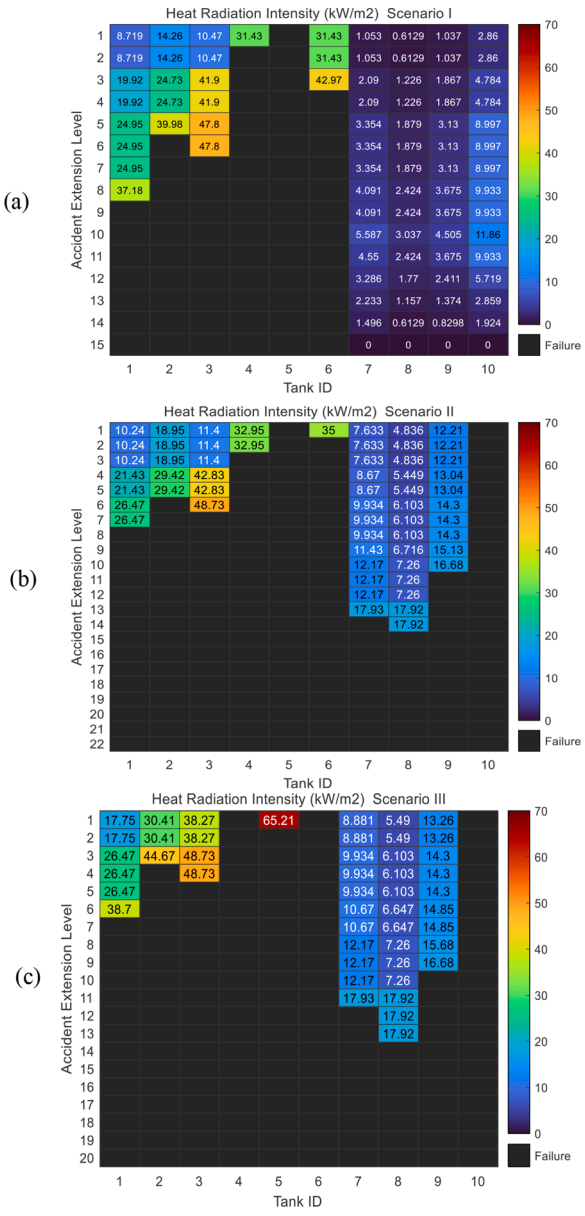

Fig. 9. Heat radiation intensity received by tanks in different accident extension levels, (a) Scenario I; (b) Scenario II; (c) Scenario III.

Table 12
System dynamic risk analysis results (Scenario I).

System Evolution Time (Min)	Critical System Units	Risk Values
$t_2 = 5.91$	Tank 4	$Risk(S_1) = 1.541\text{e}-14$
$t_3 = 5.97$	Tank 4	$Risk(S_2) = 4.958\text{e}-03$
$t_4 = 6.16$	Tank 6	$Risk(S_3) = 1.827\text{e}-12$
$t_5 = 6.45$	Tank 6	$Risk(S_4) = 1.218\text{e}-01$
$t_6 = 7.47$	Tank 2	$Risk(S_5) \approx 0$
$t_7 = 9.20$	Tank 3	$Risk(S_6) = 1.190\text{e}-17$
$t_8 = 9.86$	Tank 3	$Risk(S_7) = 1.616\text{e}-05$
$t_9 = 9.86$	Tank 1	$Risk(S_8) \approx 0$
$t_{10} = 19.76$	Tank 1	$Risk(S_9) = 2.884\text{e}-02$

5. Conclusion

Domino effects triggered by natural hazards are one of the emerging threats in CIPs. In reality, the evolution process of NHDC is very complex and associated with high uncertainty and spatio-temporal dynamics,

Table 13
System dynamic risk analysis results (Scenario II).

System Evolution Time (Min)	Critical System Units	Risk Values
$t_2 = 5.51$	Tank 6	$Risk(S_1) = 8.704e-13$
$t_3 = 5.60$	Tank 4	$Risk(S_2) = 1.778e-15$
$t_4 = 6.82$	Tank 4	$Risk(S_3) = 4.958$e-03
$t_5 = 6.94$	Tank 2	$Risk(S_4) \approx 0$
$t_6 = 7.83$	Tank 6	$Risk(S_5) = 1.218e-01$
$t_7 = 9.69$	Tank 3	$Risk(S_6) = 6.890e-16$
$t_8 = 9.81$	Tank 1	$Risk(S_7) = 7.390e-17$
$t_9 = 10.75$	Tank 1	$Risk(S_8) = 2.884e-02$
$t_{10} = 10.91$	Tank 3	$Risk(S_9) = 1.616e-05$
$t_{11} = 10.92$	Tank 9	$Risk(S_{10}) = 1.541e-19$
$t_{13} = 14.33$	Tank 9	$Risk(S_{12}) = 2.256e-02$
$t_{14} = 15.23$	Tank 7	$Risk(S_{13}) = 9.172e-13$
$t_{15} = 18.60$	Tank 8	$Risk(S_{14}) \approx 0$

Table 14
System dynamic risk analysis results (Scenario III).

System Evolution Time (Min)	Critical System Units	Risk Values
$t_2 = 2.73$	Tank 5	$Risk(S_1) = 1.012e-09$
$t_3 = 3.25$	Tank 5	$Risk(S_2) = 6.400e-01$
$t_4 = 3.83$	Tank 2	$Risk(S_3) = 1.175e-14$
$t_5 = 4.41$	Tank 3	$Risk(S_4) = 5.999e-16$
$t_6 = 5.06$	Tank 3	$Risk(S_5) = 1.616e-05$
$t_7 = 5.79$	Tank 1	$Risk(S_6) = 6.890e-16$
$t_8 = 6.19$	Tank 1	$Risk(S_7) = 3.945e-15$
$t_9 = 9.59$	Tank 9	$Risk(S_8) = 4.997e-12$
$t_{11} = 11.35$	Tank 9	$Risk(S_{10}) = 2.256e-02$
$t_{12} = 12.74$	Tank 7	$Risk(S_{11}) \approx 0$
$t_{13} = 15.94$	Tank 8	$Risk(S_{12}) \approx 0$

which brings great challenges to the prevention and mitigation of such catastrophic chain events. The involvement of natural hazards leads to a more complex and severe accident scenario. The synergistic effects associated with multiple simultaneous technological hazards can significantly accelerate the evolution of accidents. In this work, a high-efficiency and systematic analytical framework was developed to model the spatial-temporal evolution of NHDC from a macro-systemic perspective. The proposed methodology is applied to analyze a typical earthquake triggered domino scenario. The effectiveness and efficiency of the proposed methodology are verified in the Appendix.

The proposed methodology is applicable to a broad range of uncertain and time-varying factors related to NHDC, which can efficiently handle the simulation of large-scale system state transition spaces. According to the spatial-temporal characteristics of NHDC, five distinctive stages of the whole evolution process were identified: the Na-tech stage, the derivation stage, the domino stage, the deterioration stage and the extinguish stage. System dynamic risk analysis results indicate that the value of system dynamic risk is likely to surge in the deterioration stage. Protective measures should be taken as soon as possible to cut off the disaster chain. Since the evolution process is associated with significant spatio-temporal dynamic characteristics, single prevention measures cannot effectively contain the damage caused by such multi-hazard scenario. Specific prevention measures are required for each stage. Our methodology can dynamically identify the critical system temporal intervals and units at each evolution stage. Taking specific protective measures for the critical system units can effectively prevent and mitigate the loss caused by NHDC. Thus, our work can provide necessary support for preventing and mitigating the loss caused by NHDC.

Finally, it must be admitted that there are still some issues in the present study that have not yet been resolved. The proposed methodology mainly focused on the release of hazardous material caused by the structural damage of equipment. However, for a complex safety-critical system, the accident evolution can also be initiated by the unavailability of auxiliary systems and utilities available in CIPs. Capturing the cross-system propagation characteristics of failures is still a challenging work. Moreover, the reliability of the analysis results is largely limited by the adopted basic probabilistic models. Most of these existing probabilistic models were driven by analytical and numerical approximations, which may lack a clear insight into the equipment damage caused by sequential or synchronous multiple hazards.

CRediT authorship contribution statement

Jinkun Men: Conceptualization, Methodology, Software, Writing – original draft, Writing – review & editing. **Guohua Chen:** Conceptualization, Resources, Supervision, Project administration, Funding acquisition, Writing – review & editing. **Yunfeng Yang:** Conceptualization, Methodology. **Genserik Reniers:** Conceptualization, Writing – review & editing.

Declaration of Competing Interest

No conflict of interest exits in the submission of this manuscript, and manuscript is approved by all authors for publication. I would like to declare on behalf of my co-authors that the work described was original research that has not been published previously, and not under consideration for publication elsewhere, in whole or in part. All the authors listed have approved the manuscript that is enclosed.

Data availability

The authors are unable or have chosen not to specify which data has been used.

Acknowledgments

This study was supported by the National Natural Science Foundation of China (22078109), the Key-Area Research and Development Program of Guangdong Province (2019B111102001), the Department of Science and Technology of Guangdong Province (2021 Overseas Academic Specialist Program), and the China Scholarship Council (202206150061).

Supplementary materials

Supplementary material associated with this article can be found, in the online version, at doi:10.1016/j.ress.2022.108723.

References

[1] Khan F, Rathnayaka S, Ahmed S. Methods and models in process safety and risk management: past, present and future. Process Saf Environ Prot 2015;98:116–47.
[2] Men J, Chen G, Tao Z. Multi-hazard coupling effects in chemical process industry: part II research advances and future perspectives on methodologies. IEEE Syst J 2022;Early Access:1–11. https://doi.org/10.1109/JSYST.2022.3182983.
[3] Men J, Chen G, Zeng T. Multi-hazard coupling effects in chemical process industry: part I preliminaries and mechanism. IEEE Syst J 2022;Early Access:1–11. https://doi.org/10.1109/JSYST.2022.3182994.
[4] Reniers G, Khakzad N, Cozzani V, Khan F. The impact of nature on chemical industrial facilities: dealing with challenges for creating resilient chemical industrial parks. J Loss Prev Process Ind 2018;56:378–85.
[5] Showalter PS, Myers MF. Natural disasters in the United States as release agents of oil, chemicals, or radiological materials between 1980-1989: analysis and recommendations. Risk Anal 1994;14:69–182.
[6] Ricci F, Moreno VC, Cozzani V. A comprehensive analysis of the occurrence of Natech events in the process industry. Process Saf Environ Prot 2021;147:703–13.
[7] Sengul H, Santella N, Steinberg LJ, Cruz AM. Analysis of hazardous material releases due to natural hazards in the United States. Disasters 2012;36:723–43.
[8] Khakzad N, Van Gelder P. Vulnerability of industrial plants to flood-induced Natechs: a Bayesian network approach. Reliab Eng Syst Saf 2018;169:403–11.
[9] Kumasaki M, King M. Three cases in Japan occurred by natural hazards and lessons for Natech disaster management. Int J Disaster Risk Reduct 2020;51:101855.
[10] Jiang P, Men J, Xu H, Zheng S, Kong Y, Zhang L. A variable neighborhood search-based hybrid multiobjective evolutionary algorithm for HazMat heterogeneous vehicle routing problem with time windows. IEEE Syst J 2020;14:4344–55.

[11] Lan M, Gardoni P, Qin R, Zhang X, Zhu J, Lo S. Modeling Natech-related domino effects in process clusters: a network-based approach. Reliab Eng Syst Saf 2022; 221:108329.
[12] Huang K, Chen G, Yang Y, Chen P. An innovative quantitative analysis methodology for Natech events triggered by earthquakes in chemical tank farms. Saf Sci 2020;128:104744.
[13] Camila SPM, Mathis P, Felipe M, Maria CA. Systematic literature review and qualitative meta-analysis of Natech research in the past four decades. Saf Sci 2019; 116:58–77.
[14] Ruckart PZ, Orr MF, Lanier K, Koehler A. Hazardous substances releases associated with hurricanes Katrina and Rita in industrial settings, Louisiana and Texas. J Hazard Mater 2008;159:53–7.
[15] Laurent A, Pey A, Gurtel P, Fabiano B. A critical perspective on the implementation of the EU council *Seveso Directives* in France, Germany, Italy and Spain. Process Saf Environ Prot 2021;148:47–74.
[16] Krausmann E, Cruz AM, Salzano E. Reducing the risk of natural-hazard impact on hazardous installations. Netherlands: Elsevier; 2017.
[17] Yang Y, Chen G, Genserik R. Vulnerability assessment of atmospheric storage tanks to floods based on logistic regression. Reliab Eng Syst Saf 2020;196:106721.
[18] Celano F, Dolšek M. Fatality risk estimation for industrialized urban areas considering multi-hazard domino effects triggered by earthquakes. Reliab Eng Syst Saf 2021;206:107287.
[19] Misuri A, Antonioni G, Cozzani V. Quantitative risk assessment of domino effect in Natech scenarios triggered by lightning. J Loss Prev Process Ind 2020;64:12.
[20] Zeng T, Chen G, Reniers G, Yang Y. Methodology for quantitative risk analysis of domino effects triggered by flood. Process Saf Environ Prot 2021;147:866–77.
[21] Caputo AC, Kalemi B, Paolacci F, Corritore D. Computing resilience of process plants under Na-Tech events: methodology and application to sesmic loading scenarios. Reliab Eng Syst Saf 2020;195:106685.
[22] Misuri A, Landucci G, Cozzani V. Assessment of safety barrier performance in the mitigation of domino scenarios caused by Natech events. Reliab Eng Syst Saf 2021; 205:107278.
[23] Chen G, Zou M. Coupling relationship model of multi-hazard and pattern of chain-cutting disaster mitigation in chemical industry park. Chem Ind Eng Prog 2018;37: 3271–9.
[24] Chen C, Reniers G, Zhang L. An innovative methodology for quickly modeling the spatial-temporal evolution of domino accidents triggered by fire. J Loss Prev Process Ind 2018;54:312–24.
[25] Cozzani V, Gubinelli G, Antonioni G, Spadoni G, Zanelli S. The assessment of risk caused by domino effect in quantitative area risk analysis. J Hazard Mater 2005; 127:14–30.
[26] Huang K, Chen G, Khan F, Yang Y. Dynamic analysis for fire-induced domino effects in chemical process industries. Process Saf Environ Prot 2021;148:686–97.
[27] Chen C, Reniers G, Khakzad N. A dynamic multi-agent approach for modeling the evolution of multi-hazard accident scenarios in chemical plants. Reliab Eng Syst Saf 2021;207:107349.
[28] Nima K, Reniers G. Using graph theory to analyze the vulnerability of process plants in the context of cascading effects. Reliab Eng Syst Saf 2015;143:63–73.
[29] Ovidi F, Zhang L, Landucci G, Reniers G. Agent-based model and simulation of mitigated domino scenarios in chemical tank farms. Reliab Eng Syst Saf 2021;209: 107476.
[30] Men J, Chen G, Yang Y. A macro-systematic accident propagation analysis for preventing natural hazard-induced domino chain in chemical industrial parks. Chem Eng Trans 2022;90:169–74.
[31] Kamil MZ, Taleb-Berrouane M, Khan F, Ahmed S. Dynamic domino effect risk assessment using Petri-nets. Process Saf Environ Prot 2019;124:308–16.
[32] Zeng T, Chen G, Yang Y, Chen P, Reniers G. Developing an advanced dynamic risk analysis method for fire-related domino effects. Process Saf Environ Prot 2020;134: 149–60.
[33] Peng Z, Hu J, Luo R, Ghosh BK. Distributed multi-agent temporal-difference learning with full neighbor information. Control Theory Technol 2020;18:379–89.
[34] Chi S, Han S. Analyses of systems theory for construction accident prevention with specific reference to OSHA accident reports. Int J Proj Manag 2013;31:1027–41.
[35] Landucci G, Gubinelli G, Antonioni G, Cozzani V. The assessment of the damage probability of storage tanks in domino events triggered by fire. Accid Anal Prev 2009;41:1206–15.
[36] Vílchez JA, Espejo V, Casal J. Generic event trees and probabilities for the release of different types of hazardous materials. J Loss Prev Process Ind 2011;24:281–7.
[37] Chen C, Reniers G, Khakzad N. A thorough classification and discussion of approaches for modeling and managing domino effects in the process industries. Saf Sci 2020;125:104618.
[38] Cozzani V, Gubinelli G, Salzano E. Escalation thresholds in the assessment of domino accidental events. J Hazard Mater 2006;129:1–21.
[39] Baalisampang T, Abbassi R, Garaniya V, Khan F, Dadashzadeh M. Modelling an integrated impact of fire, explosion and combustion products during transitional events caused by an accidental release of LNG. Process Saf Environ Prot 2019;128: 259–72.
[40] Reniers G, Cozzani V. Domino effects in the process industries, modeling, prevention and managing. Amsterdam, The Netherlands: Elsevier; 2013.
[41] Liang Q, Yang Y, Zhang H, Peng C, Lu J. Analysis of simplification in Markov state-based models for reliability assessment of complex safety systems. Reliab Eng Syst Saf 2022;221:108373.
[42] Campedel M, Cozzani V, Garcia-Agreda A, Salzano E. Extending the quantitative assessment of industrial risks to earthquake effects. Risk Anal 2008;28:1231–46.
[43] Ronza A, Vílchez JA, Casal J. Using transportation accident databases to investigate ignition and explosion probabilities of flammable spills. J Hazard Mater 2007;146:106–23.